Supporting Information: Physical Vapor Deposition Features of Ultrathin Nanocrystals of $Bi_2(Te_xSe_{1-x})_3$

Dmitry S. Yakovlev,[†,‡] Dmitry S. Lvov,[¶] Olga V. Emelyanova,[§] Pave S. Dzhumaev,[§] Igor V. Shchetinin,[‖] Olga V. Skryabina,[†,¶] Sergey V. Egorov,[‡,¶] Valery V. Ryazanov,[‡,¶] Alexander A. Golubov,[†,⊥] Dimitri Roditchev,[#] and Vasily S. Stolyarov[*,†,@,‖]

†*Center for Advanced Mesoscience and nanotechnology, Moscow Institute of Physics and Technology, Dolgoprudny 141700 Moscow, Russia*

‡*Russian Quantum Center, Skolkovo, Moscow Region, 143025, Russia*

¶*Institute of Solid State Physics RAS, 142432 Chernogolovka, Russia*

§*National Research Nuclear University MEPhI, 115409 Moscow, Russia*

‖*National University of Science and Technology MISIS, 119049 Moscow*

⊥*Faculty of Science and Technology and MESA+ Institute of Nanotechnology, 7500 AE Enschede, The Netherlands*

#*Laboratoire de Physique et d'Étude des Matériaux (LPEM), UMR-8213, ESPCI Paris, PSL Research University, CNRS, Sorbonne Université, 75005 Paris, France*

@*Dukhov Research Institute of Automatics (VNIIA), 127055 Moscow, Russia*

E-mail: stolyarov.vs@phystech.edu

Supporting Information Available

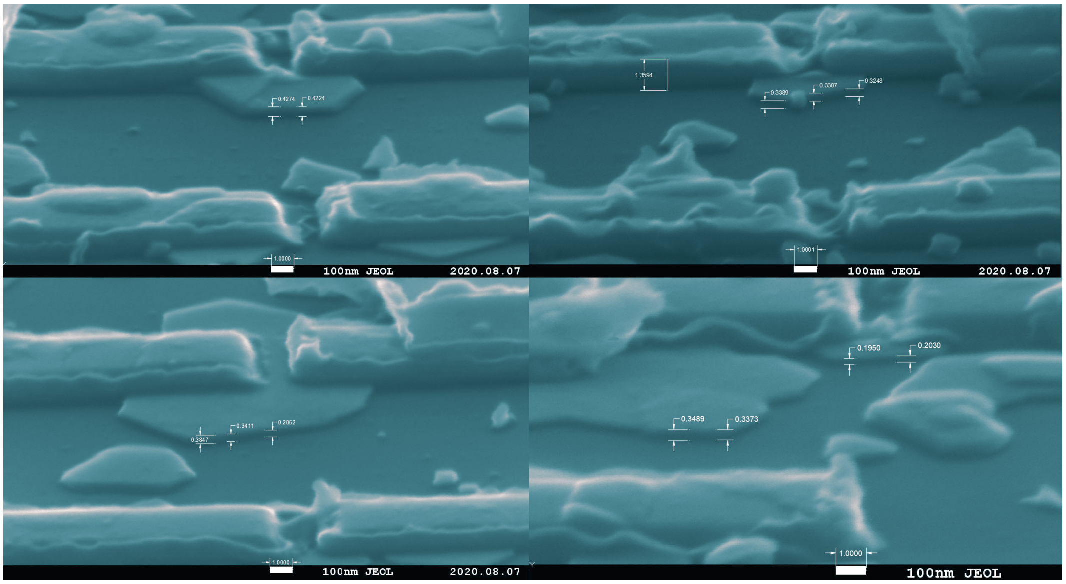

Supplementary Figure 1: SEM image of a sample for thickness measurement.The top and bottom surface of TI are indicated with the upper and lower white lines, respectively.

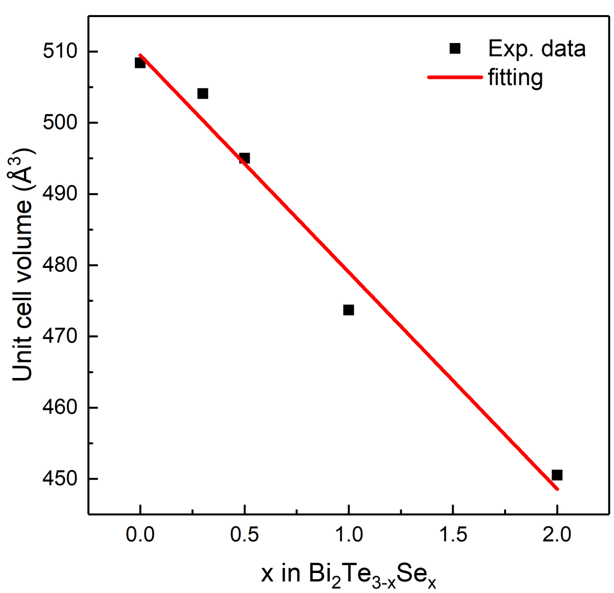

Supplementary Figure 2: The dependence of Unit cell volume on the substitution ratio of Se atoms obtained from Vegard's law. The solid line represent the lattice parameters calculated from Vegard's law.[1]

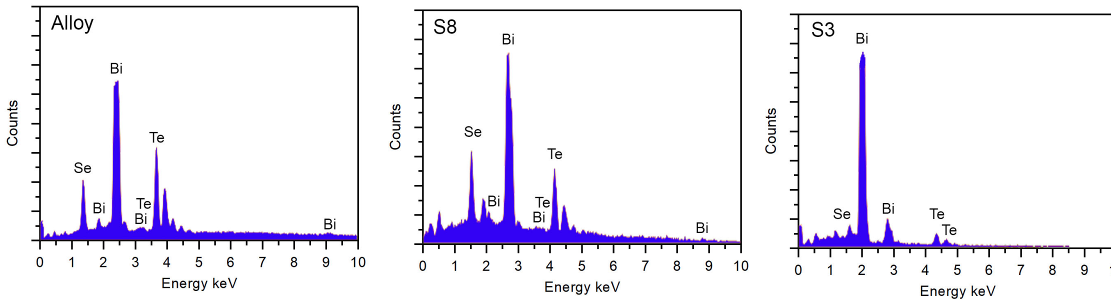

Supplementary Figure 3: Typical Energy Dispersive X-RAY spectroscopy of $Bi_2(Te_{1-x}Se_x)_3$ nanoplate.

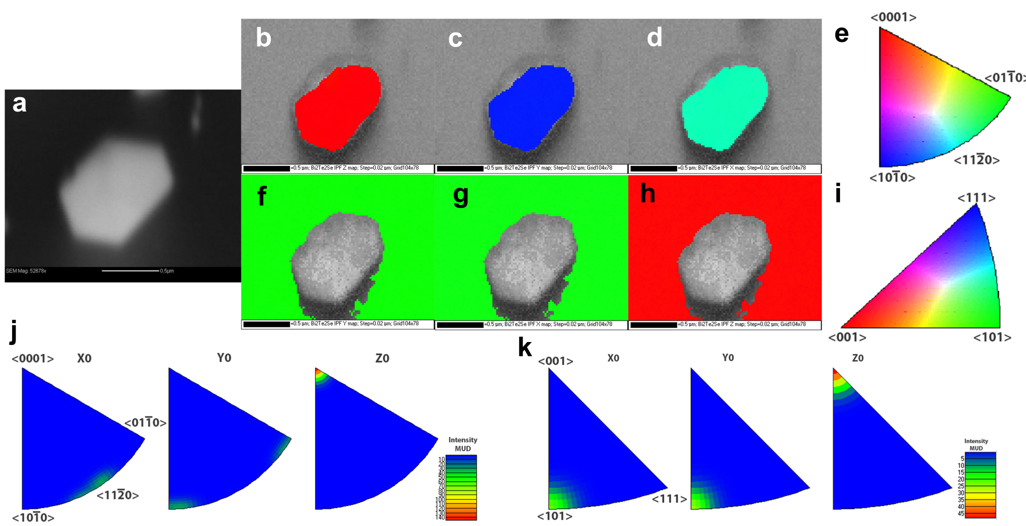

Supplementary Figure 4: **Electron backscatter diffraction. a:** SEM image (obtained with the EBSD system) of $Bi_2(Te_{1-x}Se_x)_3$ nanoplate on Si substrate located outside of Nb-electrodes **b-d:** EBSD crystallographic orientation mappings of $Bi_2(Te_{1-x}Se_x)_3$ using nverse pole figure (IPF-X, IPF-Y, and IPF-Z), respectively. **e:** Color code for the mappings in (b-d). **f-h:** EBSD crystallographic orientation mappings of Si substrate using IPF-X, IPF-Y, and IPF-Z, respectively. (i) Color code for the mappings in (f-h). **j:** EBSD inverse pole figure (IPF) of the $Bi_2(Te_{1-x}Se_x)_3$ nanoplate along X, Y, and Z directions, respectively. **r:** EBSD inverse pole figure (IPF) of the Si subsrate along X, Y, and Z directions, respectively .

References

1. Denton, Alan R., and Neil W. Ashcroft. Vegard's law. *Physical review A* **43.6** (1991): 3161.

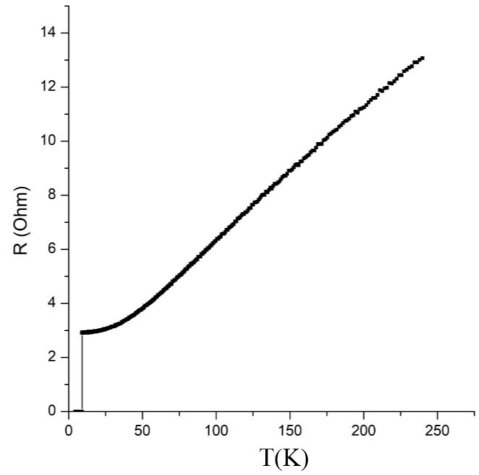

Supplementary Figure 5: Independent 4-point R(T) measurements of our 140nm thick Nb film.

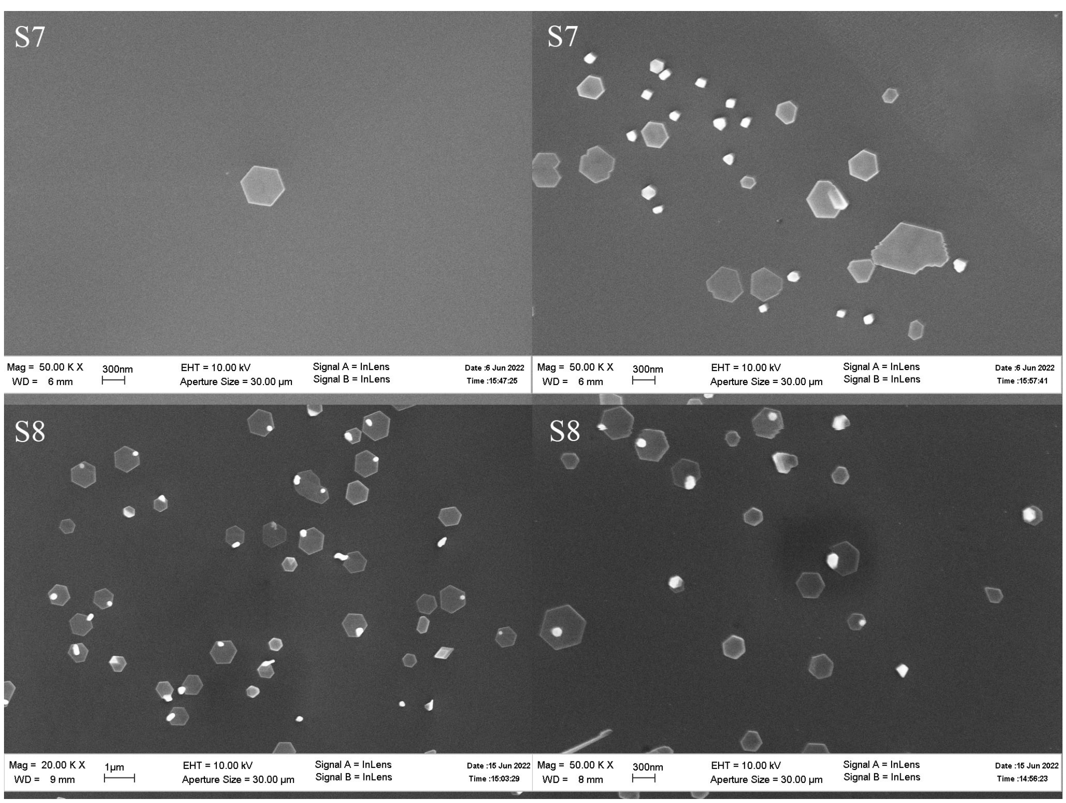

Supplementary Figure 6: SEM images of samples S7 and S8.